

Radio observations of the young planetary nebula NGC 6302

L. F. Rodríguez, J. A. García-Barreto, J. Cantó,
M. A. Moreno, S. Torres-Peimbert, R. Costero
and A. Serrano *Instituto de Astronomía Universidad Nacional Autónoma de
México Apdo. Postal 70–264, 04510, México, DF, México*

J. M. Moran *Harvard-Smithsonian Center for Astrophysics, 60 Garden St.,
Cambridge, Massachusetts USA and Radio Astronomy Laboratory, University of
California, Berkeley, California USA*

G. Garay *European Southern Observatory, Karl-Schwarzschild-Strasse 2, D-8046,
Garching Bei Munchen, FRG*

Accepted 1985 February 7. Received 1985 January 3

Summary. We present VLA observations of the bipolar planetary nebula NGC 6302 at 2, 6 and 21 cm, in continuum emission, at 2 cm in the H76 α line and at 21 cm in the H I line. Most of the continuum emission comes from an ionized toroid with outer angular diameter of ~ 10 arcsec. This toroid may be confining the wind of the central star and contributing to the formation of the optical lobes. The H76 α recombination-line emission originates predominantly from the outer parts of the ionized volume. We discuss various effects which could account for this result. Our map of the 21-cm H I absorption feature first observed by Rodríguez & Moran shows that it arises from the dark lane observable in short optical exposures. This dark lane is the outer, neutral part of a toroid whose inner, ionized zone is detected in the continuum. We also derive the electron temperature of the ionized gas, set an upper limit to the magnetic field in the neutral gas, and estimate the distance to the nebula. The characteristics of NGC 6302 and its central star are those expected for a young planetary nebula.

1 Introduction

NGC 6302 is an emission nebula with a bipolar shape. Although it is usually classified as a planetary nebula (Perek & Kohoutek 1967), some of its characteristics are peculiar and make the classification uncertain. Minkowski & Johnson (1967) found line-splitting in the [N II] emission from the two lobes of the nebula and interpreted this as evidence of expansion, but the line-splitting disappears at the centre of the nebula, indicating that expansion is less rapid in this

region. Minkowski & Johnson also noted that, on average, the radial velocities in the eastern lobe are blueshifted by $\sim 35 \text{ km s}^{-1}$ with respect to the radial velocities in the western lobe. Elliot & Meaburn (1977) confirmed that the ionized material is not expanding in a spherically symmetric mode and proposed that the gas is flowing in four separate, major streams; two from each lobe, tilted to explain the continuous shift from negative to positive velocities between the eastern and western lobes. Meaburn & Walsh (1980a) observed wide ($\sim 800 \text{ km s}^{-1}$) wing [Ne v] emission and interpreted it as evidence of an energetic stellar wind. They also suggested that the major kinematic properties of NGC 6302 could be explained in terms of the effects of a stellar wind on a surrounding toroidal nebula. In this model (*cf.* Barral & Cantó 1981), the stellar wind creates a bipolar cavity in the surrounding cloud. The stellar wind suffers an oblique shock and is refracted, sliding along the walls of the cavities. The resulting annular streams explain the line-splitting observed at the centre of the lobes of NGC 6302. Meaburn & Walsh (1980b) and Barral *et al.* (1982) discussed the presence of complex, multiple-velocity components and suggested that NGC 6302 appears to be ‘polypolar’ rather than bipolar.

Peimbert (1978) included NGC 6302 in his type I planetary nebula classification. These nebulae have excess helium and nitrogen abundances, filamentary structure, and probably come from massive progenitors (Calvet & Peimbert 1983). Combining optical and UV data, Aller *et al.* (1981) and Barral *et al.* (1982) made new determinations of the chemical composition of this object. NGC 6302 has one of the highest helium abundances ($\text{He}/\text{H} \cong 0.18$) observed in any planetary nebulae, and its nitrogen abundance is enriched by an order of magnitude with respect to the solar abundances. Rodríguez & Moran (1982) recently reported H I associated with NGC 6302, the first detection of neutral hydrogen in a planetary nebula. They found absorption features at ~ 6 and -40 km s^{-1} and suggested that the former is due to local H I absorption and the latter to H I moving out from the centre of the source toward us. The relatively low angular resolution (~ 10 arcsec) of their observations did not allow them to make spatial maps of the absorption. Since H I has not been found in several other planetary nebulae (Zuckerman, Terzian & Silverglate 1980; Pottasch *et al.* 1982; Rodríguez & García-Barreto 1984), its presence in NGC 6302 could be a peculiarity of the source.

In this paper we present radio and optical observations that provide a more accurate picture of the geometric and kinematic characteristics of NGC 6302, as well as of its evolutionary status. In Section 2 we present the radio and optical observations, while in Section 3 we interpret these and other observations in terms of a simple model. In Section 4 we summarize our results and conclusions.

2 Observations

2.1 CARBON MONOXIDE

Although NGC 6302 is generally recognized to be a post-main-sequence object, some of its characteristics are similar to those of pre-main sequence objects. For example, it is located very close to the galactic plane ($b=1^\circ.1$), and its bipolar appearance is similar in some aspects to pre-main-sequence nebula such as S106 (*e.g.* Bally & Scoville 1982) and R Mon (*e.g.* Cantó *et al.* 1981). Association with a molecular cloud is a good indicator of pre-main-sequence nature and we have searched for the $J=1 \rightarrow 0$ rotational transition of carbon monoxide in the vicinity of NGC 6302. These observations were made with the 11-m radio telescope of the National Radio Astronomy Observatory* during 1981 January in the manner described by Rodríguez, Torrelles & Moran (1981). In the velocity range -80 to $+80 \text{ km s}^{-1}$ we found no CO emission down to a 3σ upper limit in corrected antenna temperature of $\sim 1 \text{ K}$. Since molecular clouds usually have

*The NRAO is operated by Associated Universities, Inc, under contract with the National Science Foundation.

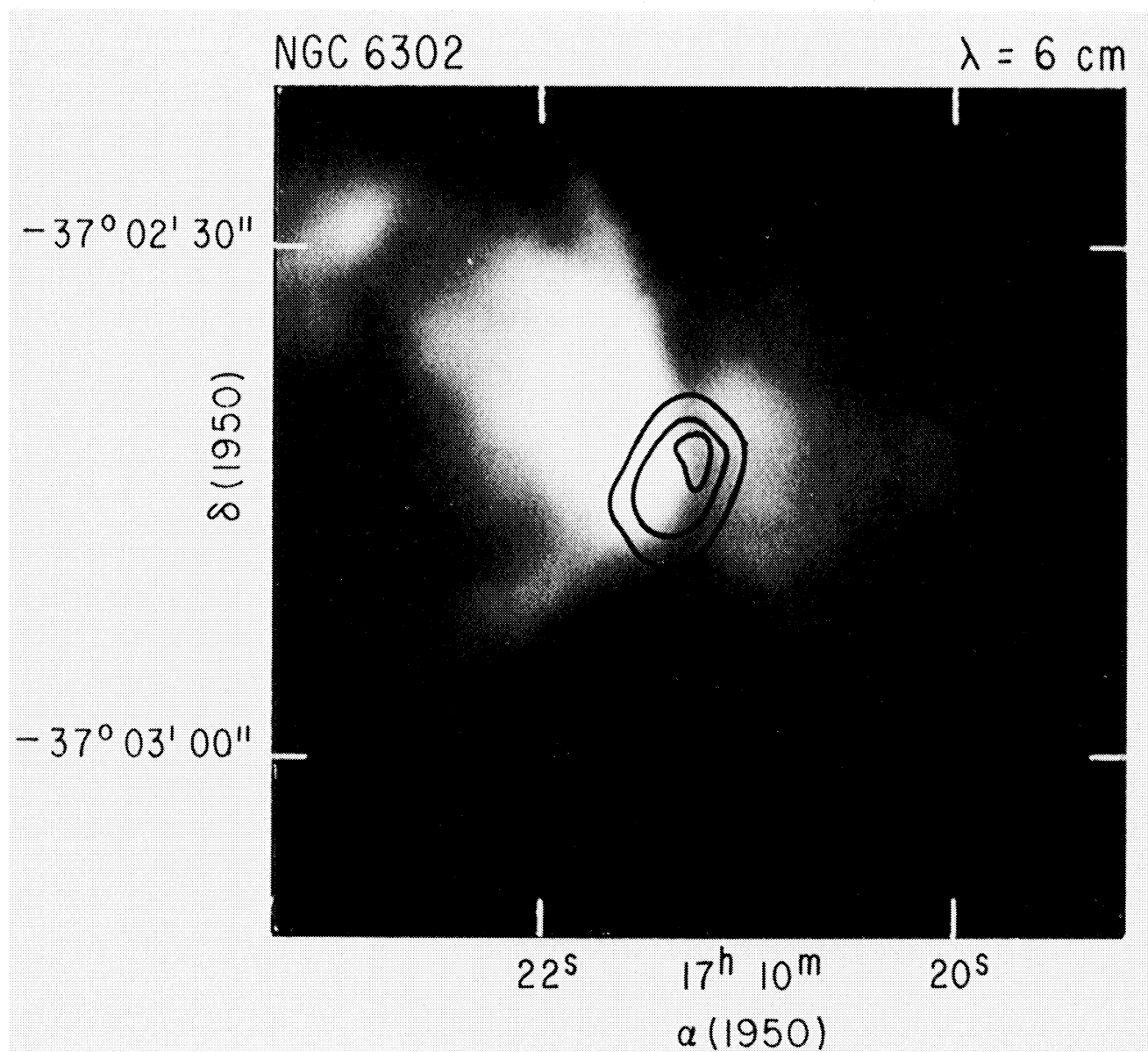


Plate 1. The 0.2, 0.5 and 0.8 contours of the 4.9-GHz map are shown here superposed on an optical photograph. The dark lane running N-S splits the core region and causes the HI absorption observed by Rodríguez, & Moran (1982).

[facing page 354]

corrected antenna temperatures of ~ 10 K, there is evidently no large molecular cloud associated with NGC 6302. It is possible to give a crude upper limit for the mass in molecular hydrogen that may exist in association with NGC 6302. We assume that any existing CO emission is optically thin, the distance is 2.0 kpc (see below), the excitation temperature is 10 K, and the linewidth is 3 km s^{-1} . For a beamsize of 66 arcsec, the usual radiative transfer formulation (*e.g.* Rodríguez *et al.* 1982a) then gives $M(\text{H}_2) \leq 0.1 M_\odot$. If the CO were in small, optically thick condensations on the other hand, the mass in molecular gas could be much larger. Our estimate is made even more uncertain because we assumed an H_2/CO ratio of 10^4 , valid for a molecular cloud but most probably not for the gas in NGC 6302 where carbon is underabundant by a factor of 4 with respect to the solar value (Aller *et al.* 1981). Furthermore, Phillips, Reay & White (1983) have detected the $2.1\text{-}\mu\text{m}$ emission of H_2 in the core of NGC 6302. Unfortunately, it is very difficult to obtain mass estimates from these lines. A search for CO in NGC 6302 using the new generation of large millimetre radio telescopes appears worthwhile, since it may be molecular line emission originating from a small region.

2.2 CONTINUUM AT 6 CM

NGC 6302 was studied interferometrically at a resolution of $2 \times 7 \text{ arcsec}^2$ at 8 GHz by Terzian, Balick & Bignell (1974) who found that, while the optical size of NGC 6302 is $\sim 1 \text{ arcmin}$, most of the radio flux comes from a compact central source. We observed NGC 6302 at 4.9 GHz using the Very Large Array of NRAO during 1980 April in the A configuration with a resolution of $\sim 0.5 \text{ arcsec}$. The procedures were those described by Rodríguez, Cantó & Moran (1982b) and the resulting map is shown in Fig. 1. The angular extent of the source is $\sim 8 \times 10 \text{ arcsec}^2$. Analysis of the fringe amplitudes as a function of interferometer spacing indicates that the flux density is $2.8 \pm 0.3 \text{ Jy}$. In Plate 1 we show some of the contours of the 6-cm continuum map superposed on a photograph taken with the 2.1-m telescope of the Observatorio Astronómico Nacional in San

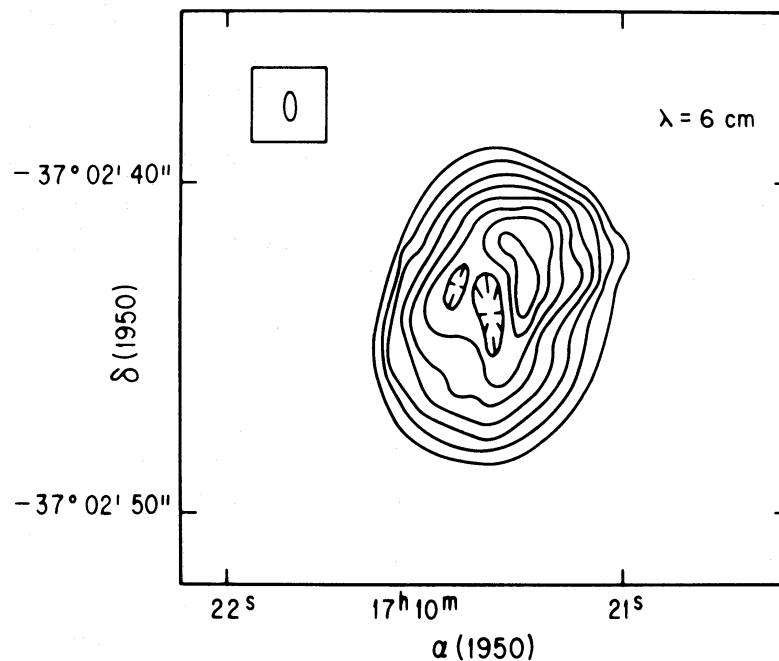


Figure 1. VLA map of NGC 6302 at 4.9 GHz. The lowest contour is 0.2 of the peak brightness 89 mJy beam^{-1} , and contour increments are 0.1 of this value. The marked contour is a decrement by the same step. Note the decrease in intensity in the central region that we interpret as evidence of a toroidal geometry.

Pedro Mártir, BC, México, made using 2415 film and a 10-min exposure time. The radio source is considerably smaller than the extended optical emission. The optical photograph also shows the dark lane running N–S suggested by Rodríguez & Moran (1982) as the origin of the H I absorption observed by them. Notice that the dark lane overlaps the brightest parts of the radio source and that it is slightly curved.

Our map also reveals a decrease in emission at the centre of the source. There are two simple source geometries which can produce a central depression in brightness, namely a shell and a toroid. A spherical shell can be ruled out since it would produce a circularly symmetric source, whereas we observe an elongated shape. We are thus left with an elliptical shell or a toroid. We favour the toroidal shape for the ionized gas because the optical data (Elliot & Meaburn 1977) suggest that existence of outflowing gas in the optical lobes. This outflow could not occur if the ionized nebula totally surrounds the central star, as expected in the case of an elliptical shell. The toroid is tilted at an angle with respect to the line-of-sight, as required by the relative blueshift of the gas in the eastern lobe with respect to the gas in the western lobe. This geometry was first proposed by Meaburn & Walsh (1980a). Our 6-cm map allows a crude estimate of the angle at which the plane of the toroid is tilted with respect to the line-of-sight. If we assume that the toroid is intrinsically circular, the observed angular dimensions of 8×10 arcsec² indicate $\sim 45^\circ$ for the angle between the plane of the toroid and the line-of-sight.

2.3 CONTINUUM AND H76 α LINE AT 2 CM WAVELENGTH

Continuum and H76 α radio recombination line observations at 14.7 GHz were made in 1984 May with the VLA in the C configuration. We observed in the spectral-line mode using 15 channels with a resolution of 8.0 km s⁻¹ after Hanning weighting. The spectral data were bandpass-normalized by the autocorrelation spectrum of each antenna and bandpass-calibrated with a strong unresolved source (3C 454.3). The continuum contribution was subtracted from the line channels using the average of four channels without evident line emission (two at each end of the spectrum). A continuum channel contained 75 per cent of the total bandwidth of 12.5 MHz. Fig. 2 shows the spectrum obtained after integrating the flux per channel in a 20×20 arcsec² region containing all the detectable continuum flux. The continuum flux density is 2.5 ± 0.1 Jy, while a Gaussian fit to the H76 α line gives $S_L = 83 \pm 7$ mJy, $\Delta v = 40 \pm 4$ km s⁻¹, and $V_{\text{LSR}} = -29 \pm 2$ km s⁻¹ for the peak flux density, full width at half maximum, and radial velocity with respect to the local standard of rest, respectively. The line width is similar to those of other planetary nebulae studied by Walmsley, Churchwell & Terzian (1981). The radio V_{LSR} is in good agreement with the optical value of -31 ± 2 km s⁻¹ (Schneider *et al.* 1983). Assuming local thermodynamic equilibrium (LTE), the average electron temperature of the nebula is

$$T_e^* = 2.99 \times 10^4 \left[\frac{S_c}{S_L \Delta v} \left(\frac{1}{1 + y^+ + 4y^{++}} \right) \right]^{0.87},$$

where y^+ and y^{++} are the number ratios of once and twice ionized helium to ionized hydrogen. From Aller *et al.* (1981), $y^+ = 0.115$ and $y^{++} = 0.065$. Using our continuum and line determinations, we obtain $T_e^* = 18000 \pm 2000$ K which is in good agreement with the range of electron temperatures determined optically, 15000 to 20000 K (Oliver & Aller 1969; Danziger, Frogel & Persson 1973; Aller & Czyzak 1978; Aller *et al.* 1981).

In the continuum we obtained the map shown in Fig. 3, very similar to that at 6 cm (Fig. 1), although its angular resolution is lower (~ 0.8 arcsec) and the central depression not as evident. The signal-to-noise ratio was insufficient to permit meaningful maps to be made of individual channels, so we averaged the data in velocity and in space. Fig. 4 shows maps of the continuum channel and the H76 α line emission in the -60 to -4 km s⁻¹ velocity range. Both maps have been

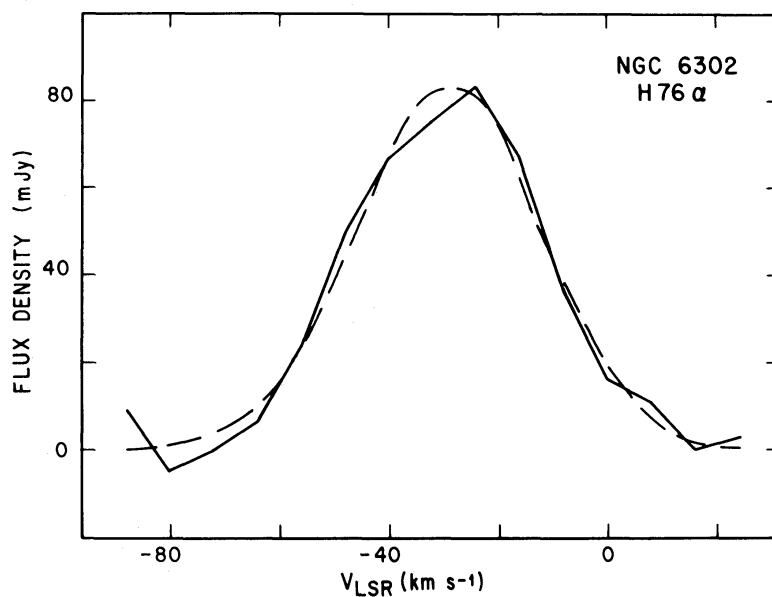


Figure 2. H76 α flux density integrated over all NGC 6302. The vertical axis is flux density and the horizontal axis is radial velocity with respect to the local standard of rest. The dashed line is a Gaussian least-squares fit to the data.

convolved with a 2×2 arcsec² Gaussian beam to improve the signal-to-noise ratio of the line map. The continuum and line maps are strikingly different, with most of the line emission coming from the NW and SE parts of the nebula. The continuum maps in Figs 1 and 3 show that these are the regions of largest emission measure. This result is similar to that found in W3(A) by van Gorkom (1980), where the H110 α line-to-continuum ratio is larger in the zones of larger emission measure. We discuss, in the following paragraphs, possible reasons for the difference between the continuum and line maps. Our analysis is similar to that by van Gorkom (1980) of W3(A).

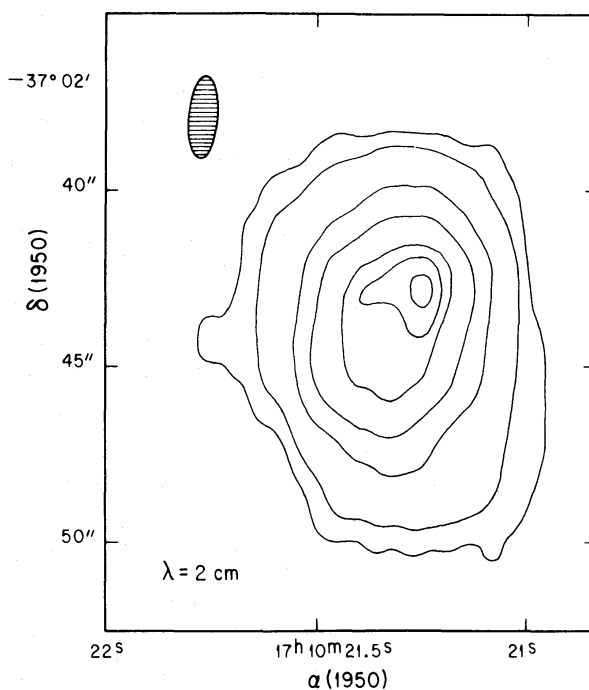


Figure 3. Cleaned VLA continuum map at 2 cm of NGC 6302. The contours are 0.05, 0.1, 0.3, 0.5, 0.75, 0.85, and 0.95 of the peak brightness of $175 \text{ mJy beam}^{-1}$. The shaded ellipse marks the solid angle contained in the half-power contour of the beam.

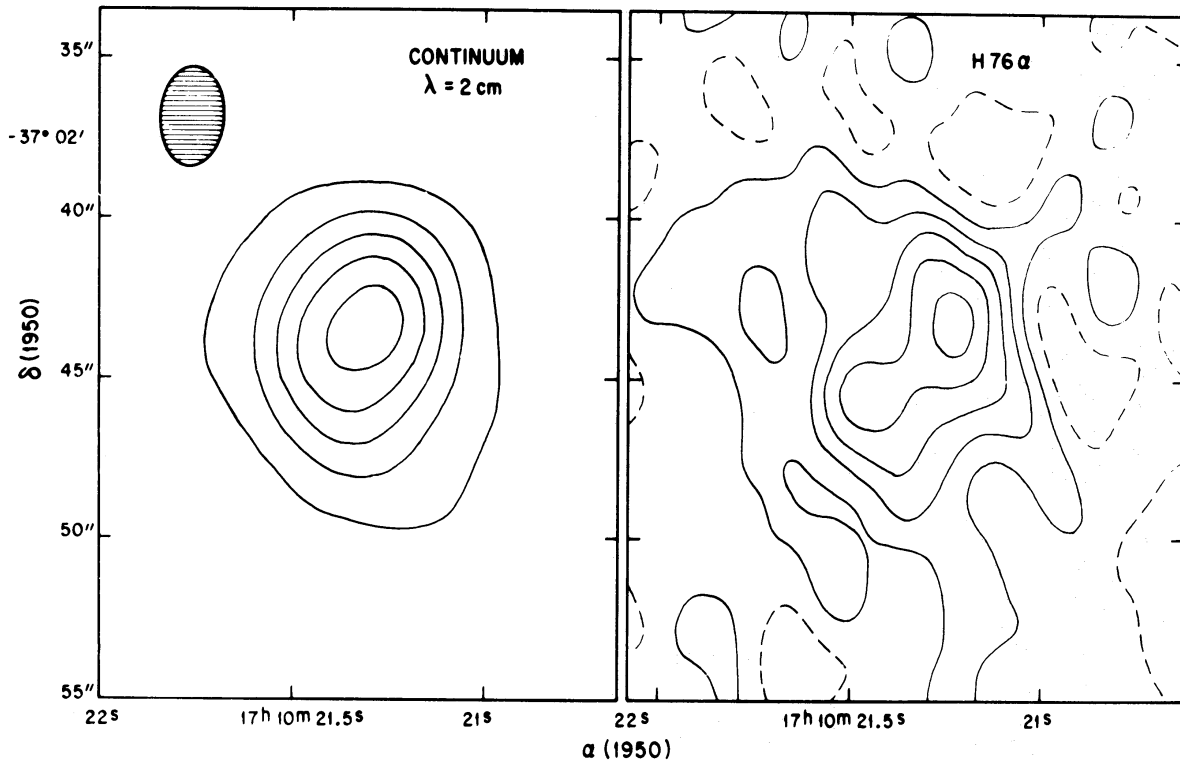


Figure 4. VLA maps of continuum (2 cm) and H76 α emission from NGC 6302. These maps have been convolved with a 2×2 arcsec² Gaussian beam to improve the signal-to-noise ratio of the line map. The contours are $-0.1, 0.1, 0.3, 0.5, 0.7$ and 0.9 of the peak brightness $470 \text{ mJy beam}^{-1}$ for the continuum map and 12 mJy beam^{-1} for the line map. The dashed ellipse marks the solid angle contained in the half-power contour of the convolved beam.

(i) *Pressure broadening of the line.* If the line were broadened significantly in the central parts of the nebula, we could not detect it in our relatively narrow bandwidth. The electron density in the core of NGC 6302 is estimated from the optical to be $\sim 2 \times 10^4 \text{ cm}^{-3}$ (Meaburn & Walsh 1980b), whereas a significant broadening of the H76 α line would require $N_e \geq 10^6 \text{ cm}^{-3}$. We conclude that pressure-broadening effects are negligible at the observed frequency. Furthermore, the regions with small line-to-continuum ratio are those of smaller emission measure, where one expects lower electron densities.

(ii) *Non-LTE departures.* The regions with largest line-to-continuum ratio are those with largest emission measure. Line emission could be stimulated in these locations. The mean emission measure and electron density for NGC 6302 are $EM \approx 2 \times 10^7 \text{ cm}^{-6} \text{ pc}$ (see Section 2.4 and $N_e \approx 2 \times 10^4 \text{ cm}^{-3}$ (Meaburn & Walsh 1980b). Fig. 5 shows the ratios of expected peak line temperature to LTE line temperature for a slab of ionized hydrogen with $T_e = 15000 \text{ K}$, $y^+ = 0.115$, $y^{++} = 0.065$, and emission measures and densities similar to the mean values for NGC 6302. These ratios were calculated following Gordon (1971). As can be seen in this figure, for low N_e and high EM we expect a line temperature enhancement of ~ 40 per cent, which could explain part of the discrepancy between the line and continuum maps. Nevertheless, to a first approximation one expects high EM s to occur in the directions of high N_e . In this case the non-LTE line enhancement will be diminished by better thermalization of the level populations. Shaver (1980) argues that this effect is responsible for the apparent LTE ratios observed in most H II regions and planetary nebulae. We conclude that non-LTE line enhancement could account for some, but not all, of the difference between the line and continuum maps.

(iii) *Different electron temperatures in the nebula.* The line emission goes as $T_e^{-1.5}$, and the continuum emission as $T_e^{-0.35}$, so if the inner region of NGC 6302 is hotter by a factor of ~ 2 than

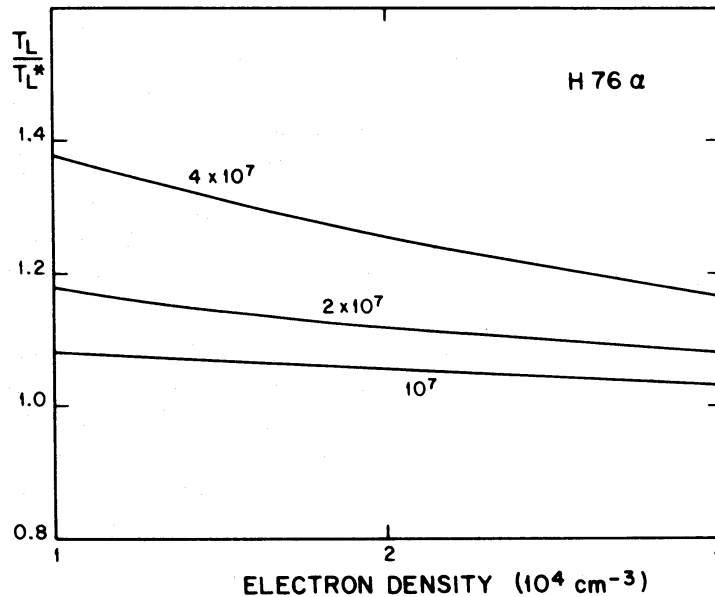


Figure 5. The ratio of line temperature to LTE line temperature, T_L/T_L^* , as a function of electron density for emission measures of 1, 2 and $4 \times 10^7 \text{ cm}^{-6}$ pc.

the outer region, we could expect this latter zone to be a substantially stronger line-emitter. However, the average electron temperature of the nebula is $\sim 18000 \text{ K}$ and it is unlikely that a photoionized plasma could reach higher T_e values (Hummer 1963). Although shock-ionized gas can reach higher electron temperatures, most of the ionization in NGC 6302 must be caused by photons from the central star. The ionization rate required by NGC 6302 is $\sim 1.0 \times 10^{48} \text{ s}^{-1}$ (see Section 3.2). We estimate the mechanical power in the wind to be $\sim 5.5 \times 10^{34} \text{ erg s}^{-1}$ (see Section 3.2). Even if we converted all this mechanical energy into ionizations, we could only provide a rate of $\sim 3 \times 10^{45} \text{ s}^{-1}$.

(iv) *Large velocity gradients in the inner part of the nebula.* if the inner parts of the nebula had large velocity gradients ($\geq 100 \text{ km s}^{-1}$), the line emission could be broadened sufficiently as to make it undetectable with the relatively narrow bandwidth used. The central star of NGC 6302 is believed to possess a powerful wind (Elliot & Meaburn 1977) which could be accelerating the inner parts of the nebula. In this case, we would expect to see broad wings in spectra of recombination lines of high signal-to-noise ratio.

(v) *The contribution to the continuum emission from twice ionized helium.* On average, NGC 6302 has $y^{++} = 0.065$ and $y^+ = 0.115$, but as a result of the stratification of the ionization structure, we expect $y^{++} \approx 0.18$ for the inner parts of the ionized toroid. Since the continuum emission is proportional to $(1 + y^+ + 4y^{++})$ the continuum-to-line ratio will be enhanced in these regions by ~ 50 per cent. This possibility can be tested by obtaining a VLA map of a He^+ recombination line. If it is correct, the He^+ line emission should fill in the regions where the $\text{H}76\alpha$ line emission is weak relative to the continuum.

In summary, we believe that non-LTE effects, velocity gradients, and the presence of large amounts of doubly ionized helium can account for the difference between line and continuum maps.

2.4 CONTINUUM AND H I LINE AT 21 CM

The 1.4-GHz observations were made with the VLA during 1982 September. At that epoch the VLA was in the B configuration and we obtained a synthesized beam of $3 \times 14 \text{ arcsec}^2$. We

observed in the spectral line mode using the central 31 of 128 channels spread across a total bandwidth of 3.125 MHz. Each channel was 24.4 kHz wide, giving a velocity resolution of 6.2 km s^{-1} for unit weighting. We used 18 antennas, the maximum allowed at that time for the chosen correlator configuration. We obtained cleaned maps for a channel free of H I absorption to derive the distribution of continuum emission from NGC 6302, and for the channel at -40 km s^{-1} where the deepest H I absorption is present. In Fig. 6 we show both maps, which are strikingly different. The continuum map reveals a source which is resolved in right ascension but not in declination, mainly because the synthesized beam is very elongated in the N-S direction. The map at the frequency of H I absorption shows two maxima.

Within the positional error (~ 1 arcsec), the depression in emission in the radio map coincides with the dark lane evident in short optical exposures, such as that shown in Plate 1 or in Evans (1959). The spatial coincidence of H I with the dark lane in NGC 6302, strengthens the argument first proposed by Rodríguez & Moran (1982) that the H I is associated with the nebula. Lester & Dinerstein (1984) recently detected an infrared disc with shape and orientation similar to the neutral toroid deduced from the H I absorption data.

Finally, analysis of the variation of fringe amplitude with interferometer spacing indicates a continuum flux density of $1.4 \pm 0.1 \text{ Jy}$ at 1.4 GHz. This value is substantially smaller than those determined at higher frequencies and suggests that the optical depth at 1.4 GHz is high. In Table 1 and Fig. 7 we present the VLA flux density measurements at 14.7, 4.9 and 1.4 GHz as well as measurements with the Parkes 64-m radiotelescope by Milne & Aller (1982), with NRAO's three-element interferometer by Terzian *et al.* (1974), and with the Molonglo Radio Telescope by

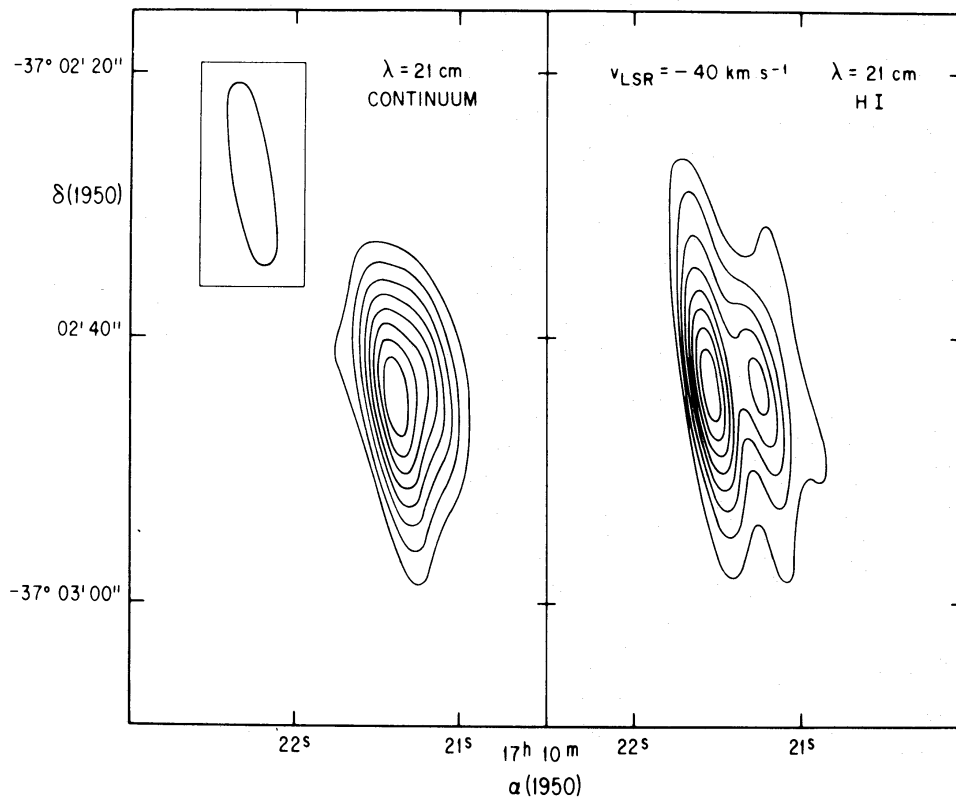


Figure 6. Cleaned VLA maps of NGC 6302 at 21 cm in continuum (left) and line (right). The line map was made for the -40 km s^{-1} absorption feature detected by Rodríguez & Moran (1982). The decrease in intensity (which corresponds to an increase in absorption) coincides spatially with the optical dark lane shown in Plate 1. The lowest contours of the continuum and line map are 0.2 of the peak brightnesses, which are 683 and $619 \text{ mJy beam}^{-1}$, respectively. The contour increments are 0.1 of the peak values.

Table 1. Continuum flux densities for NGC 6302.

<u>Frequency</u> (GHz)	<u>Flux Density</u> (Jy)	<u>Reference</u>
0.41	0.65	Calabretta 1982
1.4	1.4	This paper
2.7	2.8	Terzian <i>et al.</i> 1974
2.7	3.1	Milne & Webster 1979
4.9	2.8	This paper
5.0	3.5	Milne & Aller 1982
8.1	3.0	Terzian <i>et al.</i> 1974
14.7	3.0	Milne & Aller 1982
14.7	2.5	This paper

Calabretta (1982). The data show that the free-free emission of NGC 6302 becomes optically thin above ~ 3 GHz. All the data, with the exception of the 408-MHz measurement by Calabretta (1982), can be modelled in terms of a homogeneous source with plane-parallel geometry. The 408-MHz flux is probably dominated by the extended (~ 1 arcmin) structure observed in the visible, while the emission at frequencies higher than ~ 1 GHz comes from the radio core (~ 10 arcsec). The ionized gas in NGC 6302 has thus a core-halo structure. We assume that the flux determinations above 1 GHz refer to the bright central core and use them to model this region in terms of (for simplicity) a homogenous source with plane-parallel geometry. The thermal continuum of a plane-parallel source is given by

$$S_\nu = \frac{2 k T_e \nu^2}{c^2} \Omega [1 - \exp(-\tau_\nu)], \quad (1)$$

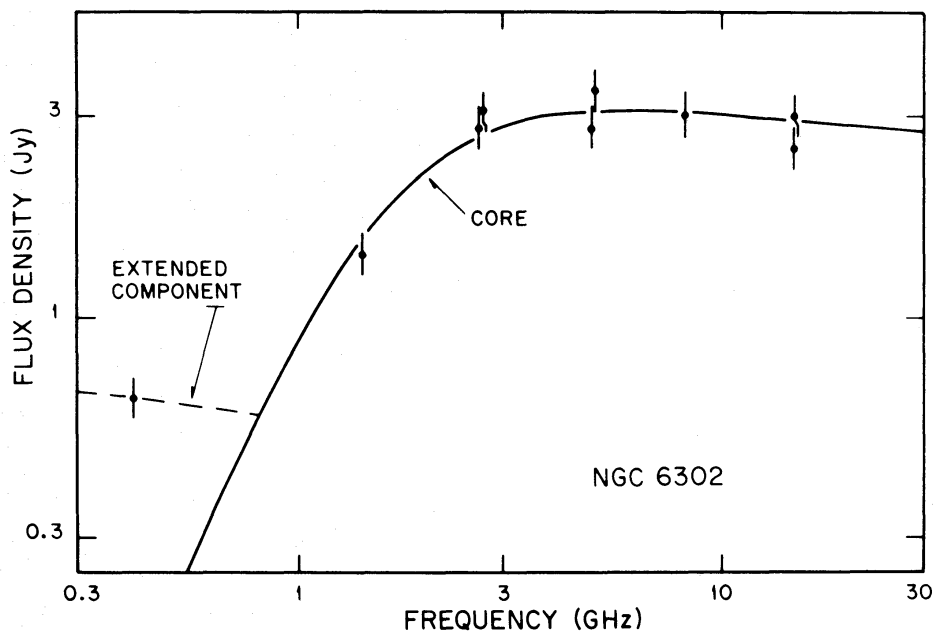


Figure 7. Radio flux density versus frequency for NGC 6302. The data above 1 GHz are well fitted with a plane-parallel model (solid line). The 408-MHz measurement by Calabretta (1983) probably refers to the extended ionized component, and is fitted with the $\nu^{-0.1}$ dependence characteristic of optically thin, ionized gas.

where k is Boltzmann's constant, T_e is the electron temperature of the ionized gas, ν is the observing frequency, c is the speed of light, Ω is the solid angle subtended by the source, and τ_ν is the optical depth at ν . The optical depth is given by

$$\tau_\nu = 0.33 \left[\frac{N_e N_p L}{10^6 \text{ cm}^{-6} \text{ pc}} \right] \left[\frac{T_e}{10^4 \text{ K}} \right]^{-1.35} \left[\frac{\nu}{\text{GHz}} \right]^{-2.1} (1 + y^+ + 4y^{++}), \quad (2)$$

where N_e and N_p are the electron and proton number densities, L is the physical depth of the source, and y^+ and y^{++} are the He^+/H^+ and $\text{He}^{++}/\text{H}^+$ ratios. We further assume that the core of NGC 6302 can be modelled as an elliptical source of projected angular dimensions of $8 \times 10 \text{ arcsec}^2$ and of constant physical depth and excitation temperature. A least-squares fit to the flux determinations above 1 GHz gives $T_e = 21\,000 \pm 5\,000 \text{ K}$, and $EM = (1.5 \pm 0.4) \times 10^7 \text{ cm}^{-6} \text{ pc}$. This electron temperature agrees well with the average H76 α value and with the range of temperatures determined optically (15 000 to 20 000 K). The large electron temperature and the presence of substantial amounts of doubly ionized helium $y^{++} \approx 0.065$ (Aller *et al.* 1981), suggest that the central star, yet undetected, must be very hot. From the helium measurements of Aller *et al.* (1981) and the results by Harman & Seaton (1966), we estimate an effective temperature of $\sim 200\,000 \text{ K}$ for the central star of NGC 6302.

2.5 AN UPPER LIMIT FOR THE MAGNETIC FIELD IN NGC 6302

The structures of some planetary nebulae could be determined by magnetic fields. We tried to find the magnetic field strength in the H I gas near NGC 6302 by measuring the Zeeman effect in the 21-cm H I line, using the VLA in the B configuration during 1982 October. We observed in the spectral-line mode using the central 128 channels of 256 distributed across a 1.5625-MHz bandwidth. The width of each channel was 6.104 kHz and the velocity resolution after Hanning weighting was 2.58 km s^{-1} . The selection of 128 channels limited the number of antennas to only nine. The synthesized beam had angular dimensions of $\sim 4 \times 10 \text{ arcsec}^2$. We observed the source during two consecutive days for periods of about 4 h. Currently in the spectral-line mode the VLA can be used in one polarization at a given time. We observed the right (R) and left (L) circular polarizations in the following repetitive sequence during the first day, RLLRLLLR, switching the polarization by means of the transfer switch which interchanged receivers. Since we always observed with the same receiver, instrumental bandpass effects were the same for each polarization. The observations on the second day were made with the same sequence but with the polarizations interchanged. This procedure assures that one obtains a very similar uv -plane coverage in both polarizations. As a check of the system we observed the maser W3(OH); a source with high circular polarization. Fig. 8 shows the resulting NGC 6302 spectrum obtained from averaging both circular polarizations. This spectrum is very similar to that obtained by Rodríguez & Moran (1982), but has higher velocity resolution. Fig. 8 also shows an emission spectrum in the direction of NGC 6302 obtained from the average of the autocorrelation spectra of the nine antennas used. We assumed an average system temperature of 60 K. This emission spectrum is equivalent to what one would observe with a single 25-m antenna, that is with an angular resolution of $\sim 30 \text{ arcmin}$.

We analyzed the H I spectrum that resulted from subtracting right minus left circular polarization absorption spectra, searching for the characteristic 'S'-shaped Zeeman pattern (e.g. Heiles & Troland 1982) that a substantial magnetic field would have produced. Note that the Zeeman splitting is much less than the linewidth. The width of the S curve is constant but the amplitude is proportional to the magnetic field. The peak-to-peak amplitude, P , of the right-minus-left spectrum is $P/A = 7.5 B/W$ (Spitzer 1978), where B is the longitudinal magnetic field in mG, W is the linewidth in kHz, and A is the signal amplitude in RCP or LCP. This technique is not sensitive

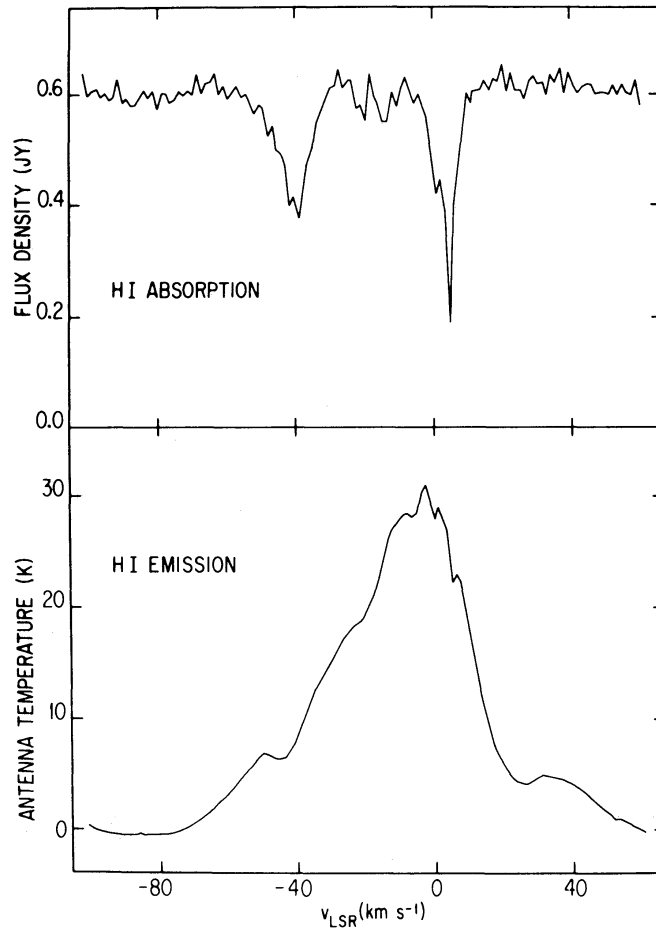


Figure 8. Absorption (top) and emission (bottom) HI spectra in the direction of NGC 6302. The angular resolutions are 4×10 arcsec² and 30 arcmin respectively.

to the transverse component of the magnetic field, which gives rise to linear polarization. That is, the right and left circularly polarized spectra would be identical for a pure transverse magnetic field. Our results, smoothed to 18 km s^{-1} for optimum detection, are shown in Fig. 9. We did not detect any significant feature above the noise and can set a 3σ upper limit of $\sim 1 \text{ mG}$ for the magnetic field strength in the neutral gas in NGC 6302. For this we have assumed that a possible magnetic field would be aligned at $\sim 45^\circ$ with the line-of-sight, on the basis of our geometric discussion in Section 2.2. Although our upper limit is not stringent, it suggests that the magnetic field is not dominant over other forms of energy in NGC 6302. The magnetic energy density is $\leq 4 \times 10^{-8} \text{ erg cm}^{-3}$. Assuming that the ionized core of NGC 6302 is characterized by an electron density of $\sim 2 \times 10^4 \text{ cm}^{-3}$ (Meaburn & Walsh 1980b) and an electron temperature of 17500 K, we estimate the thermal energy per cm^3 to be $2nkT \sim 9 \times 10^{-8} \text{ erg cm}^{-3}$. However, we cannot argue strongly that the magnetic field is dynamically unimportant in NGC 6302 since there are many uncertainties in our estimates, and the upper limit for the magnetic field refers to the neutral gas while the thermal energy density refers to the ionized gas. Limits on the Zeeman effect can be improved by a factor of 4 using the same integration time when the full spectral-line VLA is available.

2.6 THE $\text{H}\alpha/\text{H}\beta$ EMISSION LINE RATIO FROM THE LOBES

The western lobe of NGC 6302 is fainter than the eastern lobe (see Plate 1). To test if this is due to differential extinction or to an intrinsic asymmetry, we observed the brightest part of the eastern

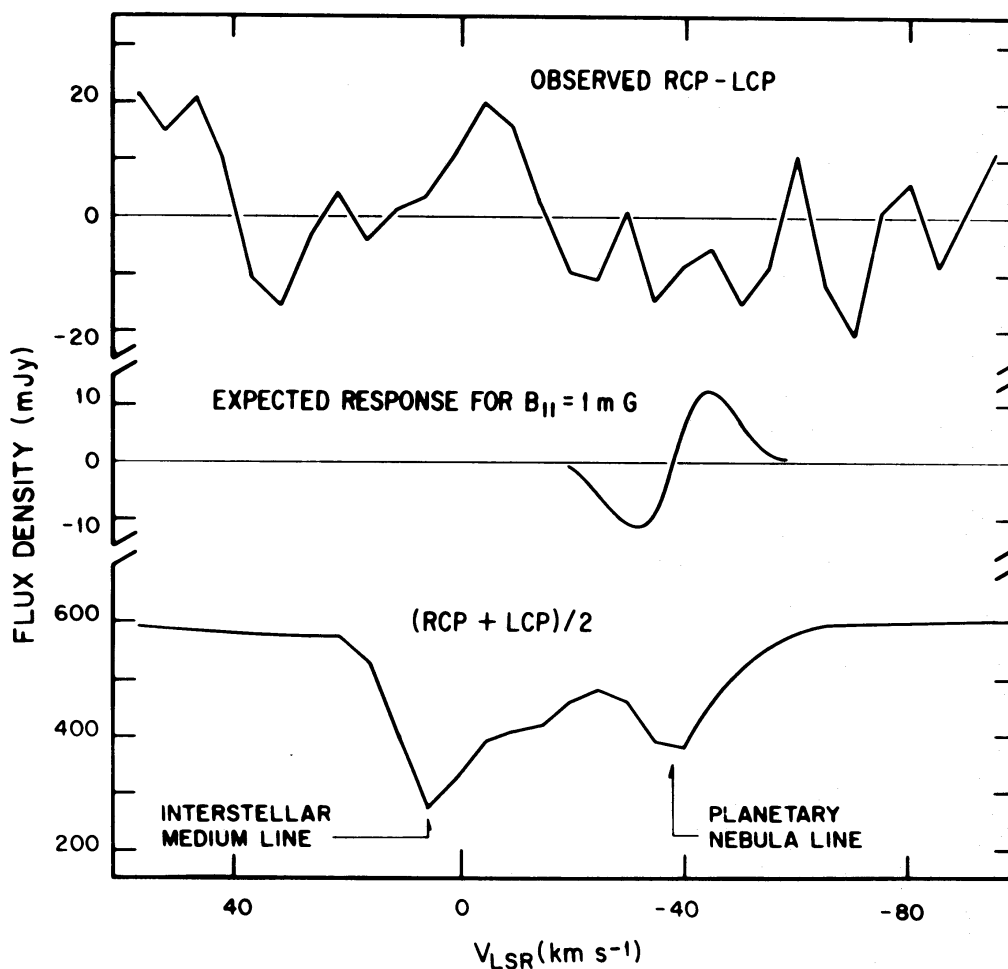


Figure 9. (Top) Spectrum obtained from the right circular polarization spectrum minus the left circular polarization spectrum. (Middle) Expected response for a longitudinal magnetic field of 1 mG. (Bottom) Average of the RCP and LPC spectra. All spectra shown in this figure are smoothed to 18 km s^{-1} .

and western lobes during 1982 July. The observations were made with the Optical Multichannel Analyzer (OMA) described by Firmani & Ruiz (1981), consisting of a WL30677 image intensifier plus a digital SIT detector. The OMA was coupled to the $f/15$ Boller and Chivens spectrograph on the 2.1-m telescope of the Observatorio Astronómico Nacional at San Pedro Mártir, BC, México. Two dispersions were used: a low one, yielding about 5.2 \AA per channel, in order to measure $H\alpha$ and $H\beta$ simultaneously in the same dispersion order, and an intermediate one, yielding about 1.9 \AA per channel, which allows us to resolve the $H\alpha$ line from the $[\text{N II}]$ doublet. The spectral regions covered in each set-up were, respectively, from 4700 to 6700 \AA and from 6400 to 6800 \AA . The fluxes were calibrated with a standard star and the wavelength scale was linearized by means of an He–Ar lamp. A large entrance slit of $7.5 \times 41 \text{ arcsec}^2$ was used, where the first value is along and the second perpendicular to the dispersion. An identical second slit 7.5 arcsec away, aligned with the first, was used alternatively for sky subtraction. The slits were oriented in the same direction of the dark lane in NGC 6302 (pa 10°). The $(H\alpha/H\beta)_{\text{WEST}}/(H\alpha/H\beta)_{\text{EAST}}$ ratio was determined to be 1.30 ± 0.07 . Since the $H\alpha/H\beta$ ratio is relatively insensitive to the nebular temperature and density conditions, we conclude that the western lobe is more reddened than the eastern lobe.

3 Discussion

3.1 A DISTANCE DETERMINATION FROM RADIO AND OPTICAL DATA

As discussed by Osterbrock (1960), the distance of a planetary nebula can be estimated from its electron density and one other quantity such as surface brightness or, correspondingly, its emission measure or its optical depth in the radiofrequency range. We will apply this method to NGC 6302, combining radio and optical data. In Section 2.4 we determined that $N_e N_p L \approx 2 \times 10^7 \text{ cm}^{-6} \text{ pc}$ for NGC 6302. From Meaburn & Walsh (1980b) we adopt an electron density of $2.0 \times 10^4 \text{ cm}^{-3}$ for the ionized core of NGC 6302. Since $N_e = N_p(1 + y^+ + 2y^{++})$, we derive $L \approx 0.04 \text{ pc}$. A reasonable estimate for the average physical depth is the radius of the nebula (5 arcsec or $\sim 2.4 \times 10^{-5} \text{ rad}$). The distance to NGC 6302 is thus simply $D \approx 0.04 \text{ pc} / 2.4 \times 10^{-5} \approx 1.7 \text{ kpc}$. This distance estimate is consistent with the value of 2.4 kpc determined by Rodríguez & Moran (1982) using the Shklovsky (1956) method. Given the uncertainties in both methods one could also argue that NGC 6302 is at 1.7 kpc, the distance to the NGC 6334 star-forming complex (Rodríguez *et al.* 1978; Neckel 1978), which is projected at only $\sim 2^\circ$ from NGC 6302. It appears reasonable to adopt a distance of about 2 kpc for NGC 6302. The consistency between the distances obtained from the electron density method and Shklovsky's method suggests that the main assumption in Shklovsky's method, that the ionized mass is $0.16 M_\odot$ for the planetary nebula, is approximately valid for NGC 6302. Rodríguez & Moran (1982) suggested that, in addition to the ionized (H II) mass of $\sim 0.16 M_\odot$, there is a neutral (H I) mass of $\sim 0.06 M_\odot$.

3.2 REMARKS ON THE CENTRAL STAR

The central star of NGC 6302 has not been detected. Its effective temperature (Section 2.4) must be very high, $\sim 200000 \text{ K}$. We can set a lower limit to the number of ionizing photons it is producing. From the nebular radio flux of 2.8 Jy at 4.9 GHz, assuming a distance of 2.0 kpc, and $T_e \approx 17500 \text{ K}$, we obtain an ionizing photon rate (Schraml & Mezger 1969) of $N_i \approx 1.0 \times 10^{48} \text{ s}^{-1}$. For comparison, an O9 ZAMS star with $L_* \approx 4.6 \times 10^4 L_\odot$ and $T_* \approx 34500 \text{ K}$ (Panagia 1973) would produce the required number of ionizing photons. Of course, we expect the central star of NGC 6302 to be less luminous but much hotter. Indeed, from the *IRAS* (1983) data, the discussion by Lester & Dinerstein (1984), and the assumption of 2 kpc for the distance, we obtain a luminosity of $L_* \approx 1.1 \times 10^4 L_\odot$ for the central star of NGC 6302. This high luminosity and the effective temperature of $\sim 200000 \text{ K}$ place it in a position in the HR diagram that is reached only by nuclei of planetary nebulae with massive progenitors (Pottasch 1983). Rodríguez & García-Barreto (1984) have argued that the presence of H I in NGC 6302 is related to the massive nature of its progenitor.

The strength of the wind can be estimated by assuming pressure balance between the wind and the ionized toroid. That is,

$$\frac{\dot{M}_* V_*}{4\pi R^2} \approx 2nkT,$$

where \dot{M}_* and V_* are the mass-loss rate and wind's terminal velocity, and R is the radius of the inner face of the toroid. From Fig. 1 we estimate for R an angular size of $\sim 1 \text{ arcsec}$ which corresponds to $3 \times 10^{16} \text{ cm}$ at 2 kpc. Thus

$$\left(\frac{\dot{M}_*}{10^{-7} M_\odot \text{ yr}^{-1}} \right) \left(\frac{V_*}{1000 \text{ km s}^{-1}} \right) \approx 1.7 \left(\frac{D}{2 \text{ kpc}} \right)^2,$$

where we have adopted $2 \times 10^4 \text{ cm}^{-3}$ and 17500 K for the electron density and temperature, respectively. This value for the rate of momentum in the wind is within the values found for other planetary nebulae (see Sabbadin *et al.* 1984, and references therein). Assuming $V_* = 1000 \text{ km s}^{-1}$, we obtain $\dot{M}_* \approx 1.7 \times 10^{-7} M_\odot \text{ yr}^{-1}$, and a mechanical power in the wind of $\sim 5.5 \times 10^{34} \text{ erg s}^{-1}$.

3.3 ARGUMENTS IN FAVOUR OF AN EXTENDED ($\sim 1 \text{ arcmin}$) LOW-DENSITY NEUTRAL HALO AROUND NGC 6302

Our radio results indicate the existence at the centre of NGC 6302 of a high-density toroidal structure with dimensions of 10 arcsec. The inner part of this toroid is ionized and can be detected by its free-free emission, while the outer part is neutral and can be detected by the H I absorption it produces in the continuum source. Of course, the extended ionized gas that gives NGC 6302 its bipolar appearance is evident in the optical. Furthermore, there are several indirect arguments that point to the existence of an extended, neutral halo not yet detected unambiguously. These arguments are the following:

(i) The bright optical lobes have well-defined edges far from the centre of the nebula. In the models by Cantó & Rodríguez (1980) and Barral & Cantó (1981), this characteristic requires the presence of an external gaseous medium that balances the ram pressure of the wind and confines sharply the extent of the stellar-wind cavities.

(ii) The mass (ionized plus neutral) of the central toroid seems to be $\sim 0.2 M_\odot$ (Rodríguez & Moran 1982), not unlike that of normal planetary nebulae. However, Calvet & Peimbert (1983) suggest that type I planetary nebulae such as NGC 6302 should have more massive envelopes. Part of the missing mass could be in the proposed neutral halo.

(iii) Danziger *et al.* (1973) find that the IR flux increases with aperture size up to $\sim 1 \text{ arcmin}$. If the IR flux is coming from heated dust, this result requires again the existence of an extended gaseous structure.

(iv) Long-exposure photographs of some planetary nebulae (Minkowski 1964; Millikan 1974; Louise 1981) show that, in addition to the bright core, there could be a fainter ionized halo. In NGC 6302, part of this halo could still be neutral.

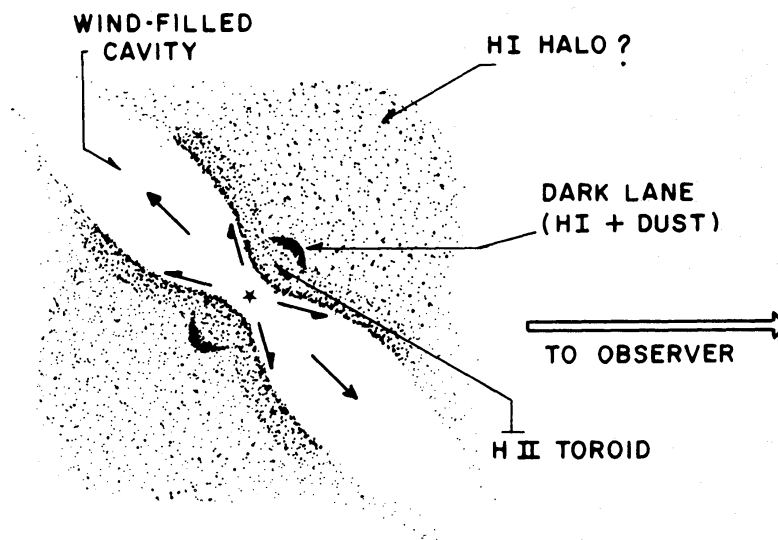


Figure 10. A schematic model of NGC 6302. The central toroid has an inner, ionized zone and an outer neutral zone. There may be a less-dense neutral halo confining the extended ionized gas.

(v) In NGC 6302, the western lobe suffers more extinction than the eastern lobe (see Plate 1 and Section 2.6). This could be explained in terms of a more extended extinction due to the halo. In Fig. 10 we present a schematic depiction of NGC 6302 which incorporates the observational results discussed in this paper.

4 Conclusions

We have studied the planetary nebula NGC 6302 with several radio techniques and reached the following conclusions.

(i) Most of the dense ionized gas in NGC 6302 is in a toroidal cloud with projected angular dimensions of $\sim 8 \times 10$ arcsec². As first proposed by Meaburn & Walsh (1980a), based on the models by Cantó (1980), this toroidal configuration must play an important role in confining the wind of the central star and in producing the lobes observable in the optical.

(ii) The line-to-continuum ratio for H7 α is larger in the outer parts of the ionized toroid. We discuss possible explanations for this effect.

(iii) The H I absorption reported by Rodríguez & Moran (1982) is probably produced by the material in the dark lane observed in short-exposure photographs. This dark lane is the outer, neutral part of the gaseous toroid whose inner ionized part produces the background free-free emission.

(iv) The recombination-line and temperature-brightness methods give an electron temperature of 15000–20000 K for the ionized gas in NGC 6302. This agrees well with optical values.

(v) The magnetic field in the neutral gas in NGC 6302 is weaker than ~ 1 mG. The magnetic energy is smaller than other forms of energy.

(vi) Both the electron density method and the Shklovsky method give a distance of ~ 2 kpc for NGC 6302.

(vii) Several observations suggest the existence of a faint neutral halo around NGC 6302, but we have no conclusive evidence concerning it.

Acknowledgements

We thank Jacqueline van Gorkom for her advice during several of the VLA runs. LFR and JC acknowledge partial support from CONACYT grant PCCBBEU020510. JAGB acknowledges support from DGAPA (UNAM).

References

- Aller, L. F. & Czyzak, S. J., 1978. *Proc. Nat. Acad. Sci.*, **75**, 1.
 Aller, L. H., Rose, J. E., O'Mara, B. J. & Keyes, C. D., 1981. *Mon. Not. R. astr. Soc.*, **197**, 95.
 Bally, J. & Scoville, N. Z., 1982. *Astrophys. J.*, **225**, 497.
 Barral, J. F. & Cantó, J., 1981. *Rev. Mex. Astr. Astrofis.*, **5**, 101.
 Barral, J. F., Cantó, J., Meaburn, J. & Walsh, J. R., 1982. *Mon. Not. R. astr. Soc.*, **199**, 141.
 Calabretta, M. R., 1982. *Mon. Not. R. astr. Soc.*, **199**, 141.
 Calvet, N. & Peimbert, M., 1983. *Rev. Mex. Astr. Astrofis.*, **5**, 319.
 Cantó, J., 1980. *Astr. Astrophys.*, **86**, 327.
 Cantó, J. & Rodríguez, L. F., 1980. *Astrophys. J.*, **329**, 982.
 Cantó, J., Rodríguez, L. F., Barral, J. F. & Carral, P., 1981. *Astrophys. J.*, **244**, 102.
 Danziger, J. J., Frogel, J. A. & Pearsson, S. E., 1973. *Astrophys. J.*, **184**, L29.
 Elliot, K. H. & Meaburn, J., 1977. *Mon. Not. R. astr. Soc.*, **181**, 499.
 Evans, D. S., 1959. *Mon. Not. R. astr. Soc.*, **119**, 150.
 Firmani, C. & Ruiz, E., 1981. *Symposium on Recent Advances in Observational Astronomy*, p. 25, eds Johnson, H. L. & Allen, C., UNAM, México.

- Gordon, M. A., 1971. *Astrophys. J.*, **167**, 21.
- Harman, R. J. & Seaton, M. J., 1966. *Mon. Not. R. astr. Soc.*, **132**, 15.
- Heiles, C. & Troland, T. H., 1981. *Astrophys. J.*, **260**, L23.
- Hummer, D. G., 1963. *Mon. Not. R. astr. Soc.*, **125**, 461.
- IRAS, 1983. *Nature*, **303**, 480.
- Lester, D. F. & Dinerstein, H. L., 1984. *Astrophys. J.*, **281**, L67.
- Louise, R., 1981. *Astr. Astrophys.*, **102**, 303.
- Meaburn, J. & Walsh, J. R., 1980a. *Mon. Not. R. astr. Soc.*, **191**, 5P.
- Meaburn, J. & Walsh, J. R., 1980b. *Mon. Not. R. astr. Soc.*, **193**, 631.
- Millikan, A. G., 1974. *Astr. J.*, **79**, 1259.
- Milne, D. K. & Aller, L. H., 1982. *Astr. Astrophys. Suppl.*, **50**, 209.
- Milne, D. K. & Webster, B. L., 1979. *Astr. Astrophys. Suppl.*, **36**, 169.
- Minkowski, R., 1964. *Publs astr. Soc. Pacif.*, **76**, 197.
- Minkowski, R. & Johnson, H. M., 1967. *Astr. Astrophys.*, **148**, 659.
- Neckel, T., 1978. *Astr. Astrophys.*, **69**, 51.
- Oliver, J. P. & Aller, J. H., 1969. *Astrophys. J.*, **157**, 601.
- Osterbrock, D. E., 1960. *Astrophys. J.*, **131**, 541.
- Panagia, N., 1973. *Astr. J.*, **78**, 929.
- Peimbert, M., 1978. In: *Planetary Nebulae, Observations and Theory, IAU Symp. No. 76*, p 215, ed. Terzian, Y., Reidel, Dordrecht, Holland.
- Perek, L. & Kohoutek, L., 1967. *Catalogue of Galactic Planetary Nebulae*, Czechoslovak Academy of Sciences.
- Phillips, J. P., Reay, N. K. & White, G. J., 1983. *Mon. Not. R. astr. Soc.*, **203**, 977.
- Pottasch, S. R., 1983. In: *Planetary Nebulae, IAU Symp. No. 103*, p. 391, ed. Flower, D. R., Reidel, Dordrecht, Holland.
- Pottasch, S. R., Goss, W. M., Arnal, E. M. & Gathier, R., 1982. *Astr. Astrophys.*, **106**, 229.
- Rodríguez, L. F. & García-Barreto, J. A., 1984. *Rev. Mex. Astr. Astrofis.*, **9**, 153.
- Rodríguez, L. F. & Moran, J. M., 1982. *Nature*, **299**, 323.
- Rodríguez, L. F., Carral, P., Ho, P. T. P. & Moran, J. M., 1982a. *Astrophys. J.*, **260**, 635.
- Rodríguez, L. F., Cantó, J. & Moran, J. M., 1982b. *Astrophys. J.*, **255**, 103.
- Rodríguez, L. F., Moran, J. M., Dickinson, D. F. & Gyulbudaghian, A. L., 1978. *Astrophys. J.*, **226**, 115.
- Rodríguez, L. F., Torrelles, J. M. & Moran, J. M., 1981. *Astr. J.*, **86**, 1245.
- Sabbadin, F., Gratton, R. G., Bianchini, A. & Ortolani, S., 1984. *Astr. Astrophys.*, **136**, 181.
- Schneider, S. E., Terzian, Y., Purgathofer, A. & Perinotto, M., 1983. *Astrophys. J. Suppl.*, **52**, 399.
- Schraml, J. & Mezger, P. G., 1969. *Astrophys. J.*, **156**, 269.
- Shaver, P. A., 1980. *Astr. Astrophys.*, **91**, 279.
- Shklovsky, I. S., 1956. *Russian Astr. J.*, **33**, 315.
- Spitzer, L., 1978. *Physical Processes in the Interstellar Medium*, p. 49, Wiley, New York.
- Terzian, Y., Balick, B. & Bignell, C., 1974. *Astrophys. J.*, **188**, 257.
- van Gorkom, J., 1980. *PhD thesis*, University of Groningen, Holland.
- Walmsley, C. M., Churchwell, E. & Terzian, Y., 1981. *Astr. Astrophys.*, **96**, 278.
- Zuckerman, B., Terzian, Y. & Silverglate, P., 1980. *Astrophys. J.*, **241**, 1014.